Supplementary Material

Antibody labelling

Recorded slices were fixed in 4% paraformaldehyde (PFA) for 1 hour at 21^{o}C with agitation. For labelling without recording, isolated cerebellum was fixed at 4°C overnight in 4% PFA, then cut into 50-100μm slices, and preincubated for 4 hrs in 0.05% Triton, 10% goat serum in phosphate buffered saline at 21^{o}C, followed by incubation with primary antibody at 21^{o}C overnight with agitation, and incubation for 8 hrs at 21^{o}C with secondary antibody. Primary antibodies were: rabbit NG2 (Chemicon, 1:200), rabbit Olig2 (gift from D. Rowitch, C.D. Stiles & J. Alberta, 1:20,000), mouse NMDA NR1 (Chemicon, 1:100), rabbit NR2A and NR2B (Chemicon, 1:50); goat NR2C and NR2D (Santa Cruz, 1:100, blocking peptides, when used, were preincubated with antibodies for 8 hours), mouse NR3A/B (Chemicon, 1:50); rabbit GFAP (DAKO, 1:500), mouse MBP (Chemicon, 1:100), mouse O4 (Chemicon, 1:40). Secondary antibodies were: goat anti-rabbit (Chemicon, 1:1500), goat anti-mouse IgG (Chemicon, 1:300), goat anti-mouse IgM Fab (Chemicon, 1:150), donkey anti-goat IgG (Molecular Probes, 1:200).

Post-embedding electron microscopic immunocytochemistry

Cerebellar tissue from adult rats (250-300g) was prepared[1]. Antibodies to GFAP (Sigma, 0.5μg/ml) and NMDA NR1 subunits (gift from R. Wenthold, 0.1μg/ml) were detected with goat anti-rabbit immunoglobulins coupled to 10nm gold particles (GAR10; British BioCell International, Cardiff). Disproving the possibility that antibody associates non-specifically with myelin, GFAP antibody was found to label astrocyte fibrils as expected but not to label myelinating processes (data not shown). Gold particle density was quantified by point counting using an overlay screen[1]: to count particles representing membrane-situated antigenic sites, immunogold particle centres and screen points within 20nm of membranes were recorded. Particle density over mitochondria in mossy fibre terminals and axon cytoplasm was negligible (Fig. 3g), showing insignificant non-specific background.

Block of glutamate- and NMDA-evoked currents by 50 and 200μM D-AP5

The incomplete block of the glutamate-evoked current by D-AP5 and NBQX in Fig. 1h,i reflects the high glutamate concentration used relative to the EC_{50} of NMDA receptors, and the fact that AP5 is a competitive blocker. In 2mM Mg in Fig. 1i, the concentrations of AP5 and NBQX used (50 and 25μM respectively) are estimated, respectively, to block (neuronal) NMDA receptors by only 39% (for 100μM glutamate, from equations 1 and 2 of ref. 2 below, using K_i=1.93μM from ref. 2 and $K_d = K_{glu}$ = 1.1μM from ref. 3) and to block (neuronal) AMPA receptors by >99% (from the K_i of 0.1μM derived in ref. 4, and the 2-site kinetic scheme and steady state K_d for glutamate of 9μM from ref. 2). By contrast, when 50μM AP5 is used to block the response to 60μM NMDA in Fig. 2h,j, it essentially abolishes the response: this reflects the fact that the NMDA concentration used is only twice the EC_{50} for NMDA (an analysis similar to that above, with a steady state K_d for NMDA of 16μM from ref. 3, predicts 95% block in this case), whereas 100μM glutamate is 40 fold higher than the EC_{50} for glutamate.

If the 19% percentage block by AP5 in 2mM Mg in Fig. 1i is scaled up by the factor of 2.56 (100%/39%) expected from the analysis above, to obtain the block that would occur if NMDA receptors were fully blocked, then the fractional contribution of NMDA receptors to the total glutamate-evoked current becomes 48% in 2mM Mg, which, when added to the 35% blocked by NBQX, accounts for 83% of the glutamate-evoked current (experimental variability and minor differences in parameters between the neuronal receptors of ref. 2 and oligodendrocyte receptors could easily account for the remaining 17% of the current).

Fig 1h,i also show data employing 200μM, rather than 50μM AP5. Analysis as above indicates that this should block NMDA receptor currents by 78% (for 100μM glutamate). In zero Mg solution we found that this blocked the 100μM glutamate-evoked current by 54%, while 25μM NBQX blocked the current by 26% (the fraction blocked by NBQX is lower than in 2mM Mg because the NMDA receptor-mediated current is 4-fold larger). As above, if we multiply the

block of 54% by 100%/78%, to obtain the block that would occur if NMDA receptors were fully blocked, we get 69% which, when added to the 26% block by NBQX, gives 95% of the current. Again we conclude that no other current contributes significantly to the glutamate-evoked current. Consistent with this, mGluR blockers did not reduce the glutamate-evoked current (Fig. 1i).

Effect of TTX and TBOA on the glutamate-evoked current

Supplementary Fig. 1 shows that blocking action potentials with TTX has no effect on the glutamate-evoked current, whereas blocking glutamate transport with TBOA increases the current (see also main Fig. 1g).

Controls for antibody labelling

Supplementary Fig. 2 shows that using blocking peptides and/or omitting the primary antibody abolishes labelling for NR1, 2C and 3 in the white matter of cerebellar slices.

Colocalization of NMDA receptor subunits in oligodendrocyte processes

Supplementary Figs. 3 and 4 show extensive overlap in labelling for NR3 and NR2C, and for NR1 and NR2C, in cerebellar oligodendrocyte processes, consistent with the receptors mediating the currents reported here containing NR1, NR2C and NR3 subunits.

Location of NR1 subunits in myelin and at the mossy fibre synapse in cerebellum

Supplementary Fig. 5A shows another example of NR1 immunogold labelling in myelin of adult rat, with the myelin slightly better preserved than in Fig. 3f. Supplementary Fig. 5B shows absence of NR1 labelling in myelin when the primary antibody is omitted. Supplementary Fig. 5C shows NR1 labelling of a mossy fibre to granule cell synapse.

Demonstration of NMDA receptor subunits in recorded cell

To demonstrate that NMDA receptor subunits are present in the recorded cells, consistent with NMDA receptors in the oligodendrocytes themselves generating the observed NMDA-evoked currents, in 3 cells we compared the distribution of Lucifer yellow introduced into the cell from the pipette, with the distribution of NR1 using immunocytochemistry. Supplementary Figure 6 shows colocalization of NR1 and Lucifer in an oligodendrocyte.

References for Supplementary Material

1. Landsend, A.S., Amiry-Moghaddam, M., Matsubara, A., Bergersen, L., Usami, S., Wenthold, R.J. & Ottersen, O.P. Differential localization of delta glutamate receptors in the rat cerebellum: coexpression with AMPA receptors in parallel fiber-spine synapses and absence from climbing fiber-spine synapses. *J. Neurosci.* **17**, 834-842 (1997).

2. Benveniste, M. & Mayer, M.L. Structure-activity analysis of binding kinetics for NMDA receptor competitive antagonists: the influence of conformational restriction. *Brit. J. Pharm.* **104**, 207-221 (1991).

3. Patneau, D.K. & Mayer, M.L. Structure-activity relationships for amino acid transmitter candidates acting at N-methyl-D-aspartate and quisqualate receptors. *J. Neurosci.* **10**, 2385-2399 (1990).

4 Diamond, J.S. & Jahr, C.E. Transporters buffer synaptically released glutamate on a submillisecond time scale.1997, *J. Neurosci.* **17**, 4672-4687 (1997).

Figure Legends for Supplementary Material

Supplementary Figure 1 Effect of TTX (1μM) and TBOA (200μM) on glutamate (100μM) evoked current in a mature cell.

Supplementary Figure 2 Controls for antibody labelling in the white matter of cerebellar slices. Labelling for NR2C is abolished by a blocking peptide (**a**) or omitting the primary antibody (**b**). Labelling for NR1 (**c**) and NR3 (**d**) is abolished by omitting the primary antibody.

Supplementary Figure 3 Colocalization (yellow) of NR3 (red) and NR2C subunits (green) in the myelinating processes of mature cerebellar oligodendrocytes. Arrow heads indicate points of high colocalization on one particular process. Dark areas indicated with arrows are cell nuclei. Scale bar 10μm.

Supplementary Figure 4 Colocalization (yellow) of NR1 (red) and NR2C subunits (green) in myelinating processes and around the soma (arrow shows nucleus) of cerebellar oligodendrocytes. Arrow heads indicate points of high colocalization on two particular processes. Scale bar 5μm.

Supplementary Figure 5 a NR1 immunogold labelling (black dots, arrow heads, Wenthold NR1 antibody) of myelin in adult rat cerebellum. **b** Labelling is abolished when primary antibody is omitted. **c** Mossy fibre terminal postsynaptic density (PSD) labelling (see also main Fig. 3g). Scale bar 0.1μm in a, 0.25μm in b,c.

Supplementary Figure 6 Images of Lucifer fill of a recorded oligodendrocyte, NR1 labelling of the slice, and an overlay of both. Arrow heads show where processes of the cell label for NR1. Scale bar 20μm.

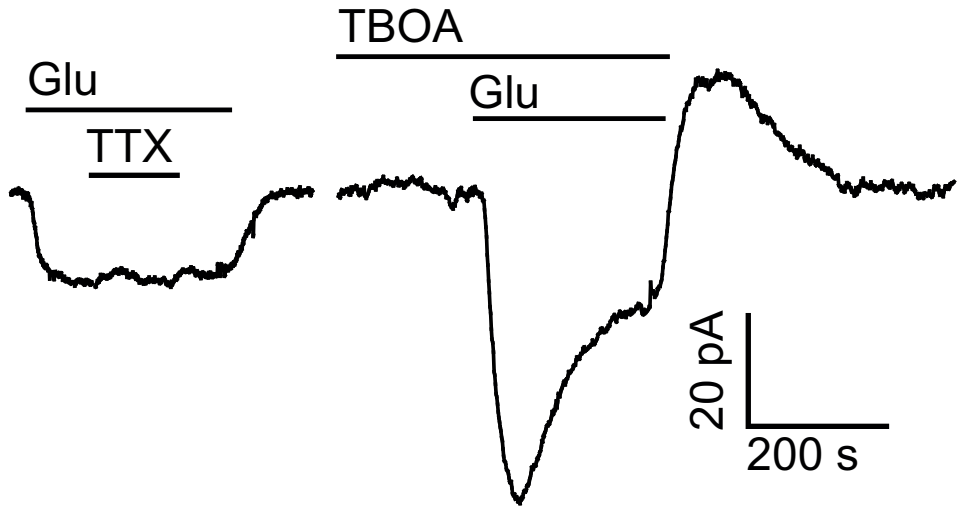

Supplementary Fig. 1

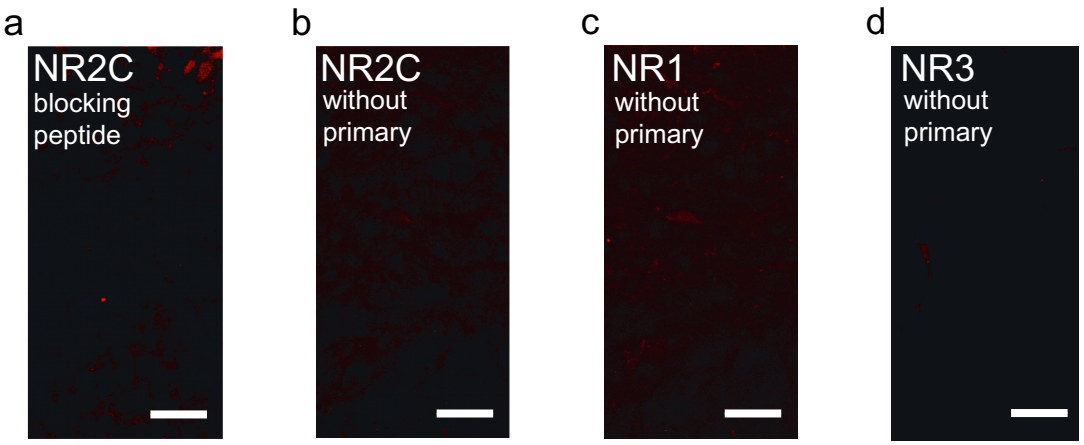

Supplementary Fig. 2

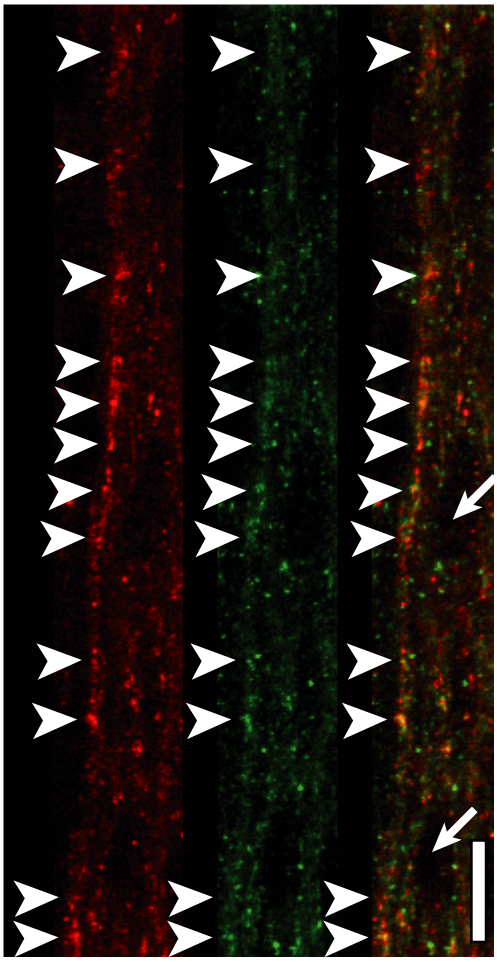

Supplementary Fig. 3

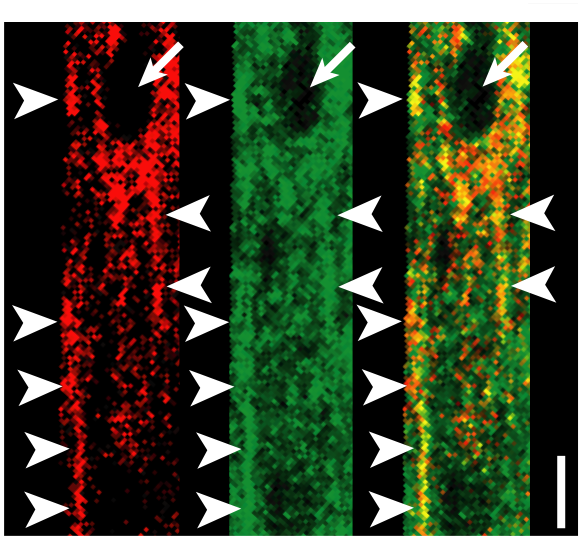

Supplementary Fig. 4

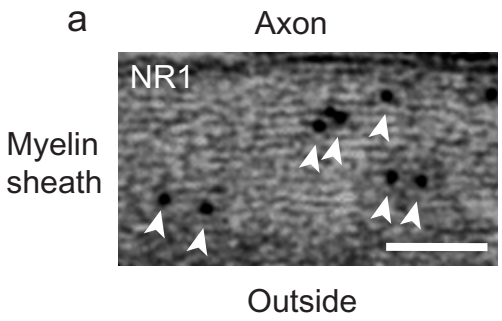

Supplementary Fig. 5

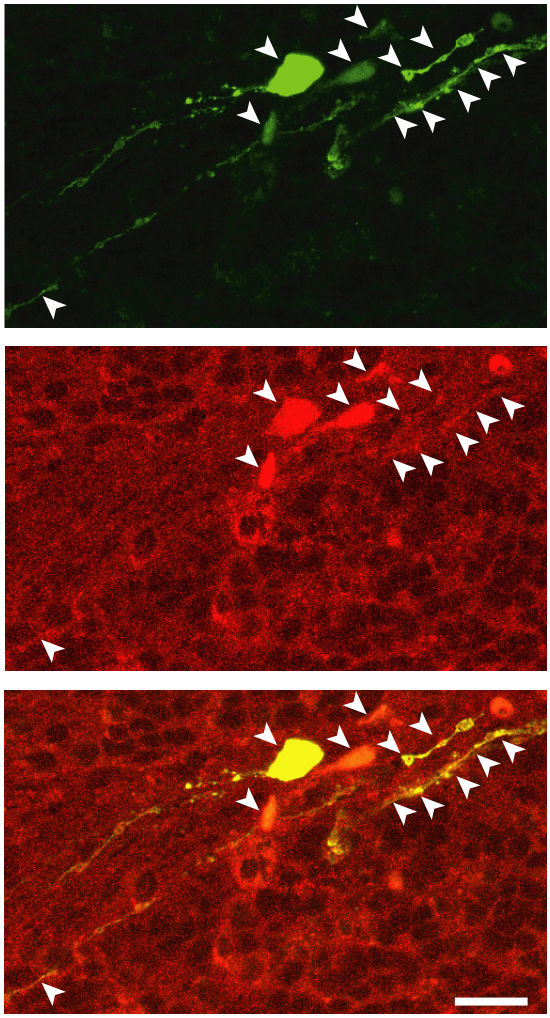

Supplementary Figure 6